forests

MDPI

Article

Spatial Variations of Soil N_2 and N_2O Emissions from a Temperate Forest: Quantified by the In Situ ^{15}N Labeling Method

Dan Xi [1,2], Yunting Fang [3,4,*] and Weixing Zhu [5]

1 Lushan Botanical Garden, Chinese Academy of Sciences, Jiujiang 332900, China
2 College of Forestry, Fujian Agriculture and Forestry University, Fuzhou 350002, China
3 CAS Key Laboratory of Forest Ecology and Management, Institute of Applied Ecology, Chinese Academy of Sciences, Shenyang 110016, China
4 Key Laboratory of Stable Isotope Techniques and Applications, Shenyang 110016, China
5 Department of Biological Sciences, Binghamton University, The State University of New York, Binghamton, NY 13902, USA
* Correspondence: fangyt@iae.ac.cn; Tel.: +86-24-83970541

Abstract: Emissions of dinitrogen (N_2) and nitrous oxide (N_2O) from soil are important components of the global nitrogen cycle. Soil N_2O emissions from terrestrial ecosystems have been well studied. However, patterns and mechanisms of N_2 emissions remain unclear due to the technical difficulty in measuring N_2 production. In this study, an in situ ^{15}N labeling method was employed to determine soil N_2 and N_2O emission rates from the lower, middle, and upper slopes, which correspond to different moisture conditions, in a temperate forest in Northeast China. We found that N_2 emissions varied from 85 to 3442 μg N m^{-2} h^{-1} across the slopes and were dominated by denitrification. The emissions of bulk N_2O (22 to 258 μg N m^{-2} h^{-1}) and denitrification-derived N_2O (14 to 246 μg N m^{-2} h^{-1}) were significantly lower than N_2 emissions from their corresponding slope positions. Both N_2 and N_2O emissions significantly increased when soils become wetter. The ratios of $N_2O/(N_2O + N_2)$ were significantly higher at the upper and middle slopes (0.22 and 0.20, respectively) compared with those at the lower slope (0.08 ± 0.01). At the catchment scale, N_2 accounted for 85% of the total gaseous N losses ($N_2O + N_2$). Our study shows that soil moisture drives the patterns of N_2 and N_2O emissions and field quantification of $N_2O/(N_2O + N_2)$ ratio should further consider the effect of slope position of forest ecosystems to estimate total soil gaseous N losses.

Keywords: ^{15}N labeling; dinitrogen emission; in situ $N_2O/(N_2O + N_2)$ ratio; temperate forest; water gradient

Citation: Xi, D.; Fang, Y.; Zhu, W. Spatial Variations of Soil N_2 and N_2O Emissions from a Temperate Forest: Quantified by the In Situ ^{15}N Labeling Method. *Forests* **2022**, *13*, 1347. https://doi.org/10.3390/f13091347

Academic Editor: Thomas H. DeLuca

Received: 11 July 2022
Accepted: 18 August 2022
Published: 24 August 2022

1. Introduction

Gaseous nitrogen (N) emissions (e.g., NO, N_2O, N_2) from soils play a crucial role in the global N cycle and climate change [1] and have been proposed as an important mechanism of terrestrial ecosystem N limitation [2]. Nitrous oxide (N_2O) and NO, as by-products of denitrification and nitrification, strongly impact global warming and atmospheric chemistry, respectively [3]. Dinitrogen (N_2), the end product of denitrification, is relatively inert in the atmosphere [4]. Compared to N_2O and NO, soil N_2 emissions have not been well-quantified due to the high background atmospheric N_2 concentration [5]. Presently, the acetylene (C_2H_2) inhibition method [6], ^{15}N isotope trace technique [7–10], and gas–flow soil core method [11–13], have all been used to determine N_2 emissions from the soil, and these methods contribute to our understanding of soil N_2 dynamics. However, at a large ecosystem scale, the field quantification of N_2 fluxes remains a huge challenge due to high spatial and temporal variations in soil environments [5,14].

Due to the above-mentioned difficulty in detecting soil N_2, the $N_2O/(N_2O + N_2)$ ratios commonly obtained from the laboratory are applied to estimate soil N_2 flux combined with

field N_2O flux [15–17]. Recently, for instance, soil N_2 flux from a maize field was calculated based on laboratory-quantified $N_2O/(N_2O + N_2)$ ratios, in situ measured N_2O emission rate, and soil factors [13]. However, some studies indicated that the physical transport of N_2O and N_2 from soil to the atmosphere in the laboratory incubation system did not realistically reflect in situ conditions [18–20]. This is because field soil environment is highly variable, where oxygen (O_2) concentration, available substrates, and other soil properties change both spatially and temporally. Additionally, the changes in soil properties have different effects on the emissions of N_2 and N_2O [21–23], consequently affecting $N_2O/(N_2O + N_2)$ ratios. Two previous studies suggested a wide range of $N_2O/(N_2O + N_2)$ ratios in the terrestrial ecosystem through a synthesis of the relevant literature [16,24]. To date, few field studies from temperate forests investigated soil $N_2O/(N_2O + N_2)$ ratios using either the acetylene inhibition method [25,26] or the ^{15}N isotope trace technique [27,28]. However, it is still unclear to researchers whether the pattern of in situ $N_2O/(N_2O + N_2)$ ratios is consistent with those in laboratory assays (i.e., Ref [9], [10] and [13]). The lack of data obtained at the field scale creates great uncertainties on the N_2 fluxes and global N cycle estimated by the existing models. Therefore, it is crucial to clarify the pattern of $N_2O/(N_2O + N_2)$ ratios in the field, which can be used as a promising tool to accurately estimate N_2 fluxes and denitrification at the ecosystem scale.

Forests cover 31.7% of global land and play a vital role in regulating the N cycle and global climates [29]. Soil N_2 and N_2O emissions are mainly mediated by microorganisms. Environmental factors, such as N and carbon (C) availability and soil moisture, influence the populations and activities of nitrifier and denitrifier, consequently causing the changes in N_2 and N_2O emissions and $N_2O/(N_2O + N_2)$ ratios [21]. Studies on factors controlling N_2O emissions from forest soils have attracted a great attention due to their global warming effect. In addition, previous studies indicated that N_2O and N_2 could be simultaneously emitted from the same soil aggregate because of the development of aerobic and anaerobic environments [13]. Thus, factors that control N_2O emissions also regulate N_2 emissions. For example, exogenous N addition in a tropical forest reduced soil N_2O emissions but had an enhancing effect on N_2 emissions under anaerobic conditions [30]; the snowmelt process promoted soil N_2 and N_2O emissions in a northern hardwood forest [9]. These studies suggest that the created anaerobic microsites in soil can enhance the proportion of denitrification to nitrification affecting the pattern of N_2 and N_2O emissions. Soil moisture may be a key driver in the development of the anaerobic conditions and the relative proportion of N_2 and N_2O emissions in the field since water controls prerequisite conditions (i.e., NO_3^- and O_2 availability) for the occurrence of nitrification and denitrification [7,31]. Moreover, topography can affect denitrification rates by changing the distribution of the substrate (NO_3^- or C) in soil water [32]. However, the effects of soil water on N_2 emissions and $N_2O/(N_2O + N_2)$ ratios remain unclear in the field under complex topography.

The purpose of the work reported was to evaluate the influence of slope position and associated soil moisture conditions on rates and ratios of N_2O and N_2 emissions in a temperate forest in Northeast China by employing an in situ ^{15}N labeling technique. The specific objectives of the study were to: (1) Use an in situ ^{15}N labeling method to determine soil N_2 and N_2O emission rates across three slopes (analogous to three moisture conditions) from a temperate forest in Northeast China; (2) explore the controlling factors of $N_2O/(N_2O + N_2)$ ratios; and (3) estimate the N_2 flux at the current ecosystem scale by measuring $N_2O/(N_2O + N_2)$ ratios and N_2O fluxes. We hypothesized that lower slopes would have greater conversion rates of N_2O to N_2 and lower $N_2O/(N_2O + N_2)$ ratios due to higher soil moisture condition.

2. Materials and Methods

2.1. Site Description

This study was conducted at the Qingyuan Forest Station (124°54′32.6″ E, 41°51′6.1″ N, 500–1100 m elevation) of Chinese Ecosystem Research Network (Qingyuan Forest CERN), located in the Liaoning Province, Northeast China (Figure 1). The climate of this region

is a continental monsoon type. In this station, the annual average precipitation from 2014 to 2020 is 666 mm with approximately 80% falling during the growing season from April to October, and the annual average temperature is 4.7 °C [33,34]. Total inorganic N deposition (TIN) in precipitation at the study site is 15 to 21 kg ha^{-1} yr^{-1} (during 2014 to 2016) with NH_4^+ contributing 65% of the N input [34,35].

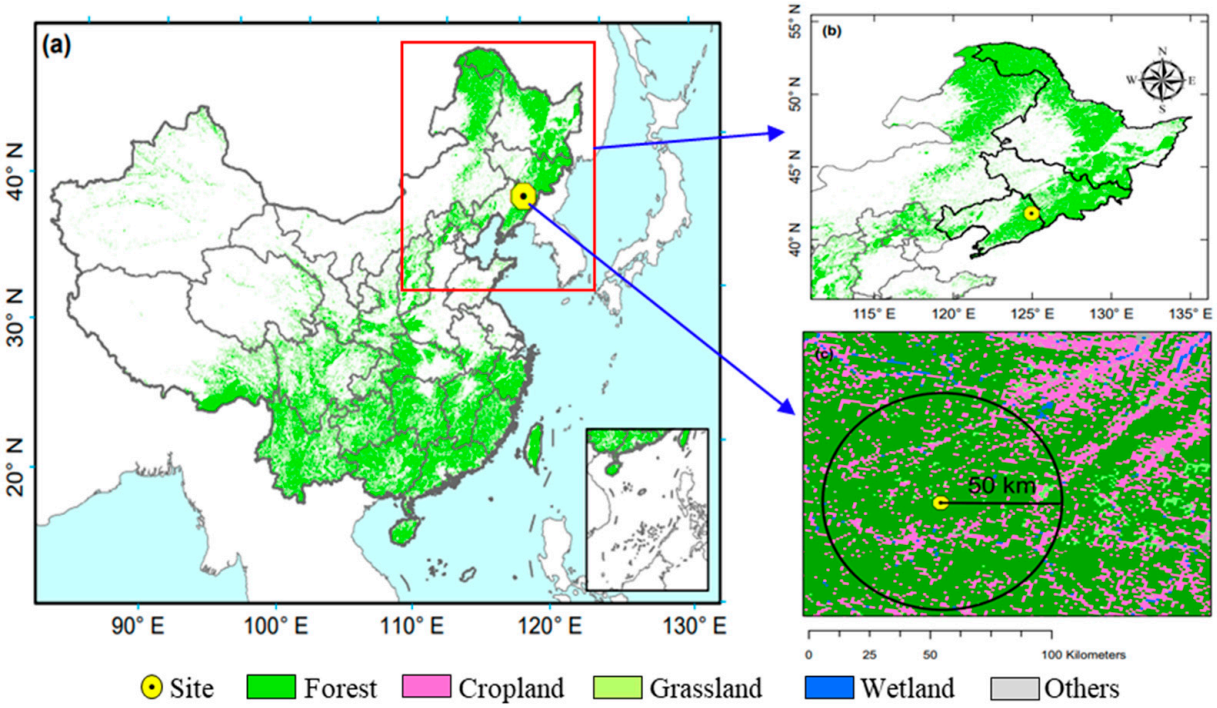

Figure 1. Location of Qingyuan Forest station in Northeast China. (**a**,**b**) present the location of Qingyuan Forest station in the map of China; (**c**) presents the main land use types within a 50-km radius of Qingyuan Forest station.

The study site was originally occupied by a primary mixed broadleaved–Korean pine forest until the 1930s. Subsequently, the original forest was destroyed by a large fire in the early 1950s and replaced by a mixture of naturally regenerating broadleaved native tree species [36]. This natural secondary forest consists of *Quercus mongolica*, *Juglans mandshurica*, *Fraxinus mandschurica*, *Phellodendron amurense*, and *Larix olgensis* in the tree layer; *Syringa amurensis*, *Acer tegmentosum*, and *Fraxinus rhynchophylla* in the understory; and *Equisetum hyemale*, *Arisaema amurense*, and *Polygonatum involucratum* in the herbaceous layer [37]. In this forest, soil with the depth of 60 to 80 cm is developed from granite gneiss and categorized into Udalfs according to the definition of the second edition of U.S. Soil Taxonomy (1999) [36]. The soil texture in 0–10 cm mineral layer is clay loam (17.2% sand, 52.8% silt, and 30% clay) with a soil pH of 5.8, bulk density (BD) of 0.70 kg m^{-3}, total organic carbon (TOC) of 2.1%, total nitrogen (TN) of 0.4%, and C/N ratio of 9.1 [34,38]. Due to the multiple effects of the topography and precipitation, the soil in lower places is usually in a water-saturated state compared with that in higher places, where soil properties can change with slope position in forests (Table 1).

Table 1. Physical–chemical properties of the 0–20 cm mineral soil layer at different slope positions in the mixed forest of Qingyuan station in Northeast China.

Slope Position	Site	Year	BD (g cm^{-3})	pH	WFPS (%)	TOC (g kg^{-1})	TN (g kg^{-1})	C/N Ratio	NH_4^+ (mg N kg^{-1})	NO_3^- (mg N kg^{-1})	NH_4^+/NO_3^- Ratio
Upper	Site 1	2015	0.60 ± 0.06 a	5.4 ± 0.0 b	36 ± 4 c	4.7 ± 0.2 b	0.47 ± 0.02 b	10.2 ± 0.1 c	2.1 ± 0.1 b	2.9 ± 0.1 a	0.7 ± 0.0 b
	Site 1	2017	0.58 ± 0.01 a	5.6 ± 0.1 a	40 ± 1 c	7.7 ± 1.3 a	0.74 ± 0.09 a	10.2 ± 0.5 a	5.9 ± 0.7 a	1.5 ± 0.2 a	3.9 ± 0.1 a
	Site 2		0.56 ± 0.01 a	5.9 ± 0.1 a	28 ± 1 c	5.8 ± 0.2 b	0.58 ± 0.01 b	9.9 ± 0.1 b	8.0 ± 0.3 a	1.7 ± 0.1 a	4.7 ± 0.2 a
	Site 3		0.60 ± 0.05 a	5.9 ± 0.1 a	40 ± 5 c	6.0 ± 0.4 a	0.62 ± 0.03 a	9.4 ± 0.1 c	6.4 ± 0.3 a	1.4 ± 0.1 a	4.7 ± 0.4 a
	Total		0.59 ± 0.02 a	5. 7 ± 0.1 a	35 ± 2 c	6.0 ± 0.4 b	0.58 ± 0.03 b	9.9 ± 0.1 b	5.3 ± 0.7 b	2.0 ± 0.2 a	3.2 ± 0.5 b
Middle	Site 1	2015	0.48 ± 0.03 a	5.6 ± 0.1 a	67 ± 4 b	5.1 ± 0.3 b	0.44 ± 0.04 b	11.7 ± 0.4 b	2.6 ± 0.8 b	2.9 ± 0.3 a	0.8 ± 0.2 b
	Site 1	2017	0.53 ± 0.02 ab	5.6 ± 0.0 a	69 ± 2 a	8.5 ± 0.8 a	1.01 ± 0.16 a	10.2 ± 0.5 a	7.4 ± 0. 9 a	1.6 ± 0.2 a	4.8 ± 1.1 a
	Site 2		0.49 ± 0.06 a	6.0 ± 0.1 a	59 ± 6 b	7.5 ± 0.9 b	0.69 ± 0.11 ab	10.8 ± 0.7 ab	9.2 ± 1.5 a	2.9 ± 0.7 a	3.8 ± 0.9 a
	Site 3		0.56 ± 0.01 a	5.8 ± 0.1 a	65 ± 3 b	8.6 ± 1.6 a	0.79 ± 0.11 a	10.4 ± 0.5 ab	9.4 ± 1.5 a	1.1 ± 0.2 a	9.4 ± 2.5 a
	Total		0.52 ± 0.02 ab	5.7 ± 0.1 a	65 ± 2 b	7.4 ± 0.6 b	0.71 ± 0.07 ab	10.8 ± 0.3 b	7.1 ± 1.0 ab	2.2 ± 0.3 a	4.7 ± 1.1 b
Lower	Site 1	2015	0.44 ± 0.07 a	5.3 ± 0.1 b	128 ± 35 a	15.0 ± 3.2 a	1.07 ± 0.18 a	13.8 ± 0.6 a	10.4 ± 1.8 a	2.0 ± 0.5 a	5.6 ± 0.9 a
	Site 1	2017	0.49 ± 0.02 b	5.5 ± 0.0 a	100 ± 5 a	9.1 ± 1.2 a	0.80 ± 0.10 a	11.4 ± 0.5 a	7.3 ± 0. 8 a	1.0 ± 0.2 a	8.1 ± 1.8 a
	Site 2		0.46 ± 0.06 a	5.9 ± 0.1 a	83 ± 8 a	10.2 ± 0.7 a	0.89 ± 0.04 a	11.5 ± 0.3 a	10.5 ± 1.8 a	1.0 ± 0.3 a	11.8 ± 1.5 a
	Site 3		0.47 ± 0.10 a	6.0 ± 0.1 a	111 ± 24 a	8.5 ± 3.3 a	0.72 ± 0.25 a	11.4 ± 0.6 a	9.1 ± 3.6 a	1.7 ± 0.5 a	6.4 ± 1.9 a
	Total		0.47 ± 0.03 b	5.7 ± 0.1 a	105 ± 9 a	10.3 ± 1.1 a	0.85 ± 0.08 a	11.9 ± 0.3 a	9.1 ± 1.0 a	1.4 ± 0.2 b	8.1 ± 1.0 a

Data are presented as mean and standard errors. Values from different sites (1, 2, 3) and overall averages are shown. Different lowercase letters indicate significant differences among slopes ($p < 0.05$).

2.2. Field ^{15}N Labeling Experiment

To determine in situ soil N_2 and N_2O emissions, static chamber and ^{15}N gas flux methods were adopted for rate measurements. In June 2015, one transect zone (site 1) along a 20 m (width) × 35 m (length) slope was chosen and divided into lower (20 m × 13 m), middle (20 m × 12 m), and upper (20 m × 10 m) slopes with three distinctive soil moisture conditions: high, intermediate, and low, respectively (Figures 2 and S1). At each slope zone, four 2 m × 3 m plots were randomly established, and a collar of stainless steel (basal area 0.09 m^2, 30 cm × 30 cm) was randomly anchored into the soil at 10 cm depth in each plot (Figure 2). All collars were finished one week before soil ^{15}N labeling. The collar had a square groove of 3 cm × 3 cm depth for matching the stainless steel chambers, and the square groove could provide a gas-tight seal when filled with water. The chambers were equipped with a 3-way sampling port and a 3 mm diameter pressure equilibration tube (15 cm long) on the preinstalled frames. Solutions of labeled $Na^{15}NO_3$ (99.26 atom% ^{15}N, Shanghai Research Institute of Chemical Industry, Shanghai, China) were evenly injected into the soil within the collars at a rate of 2.5 g ^{15}N m^{-2} (diluted in 900 mL DI water, through 144 injections) by a syringe with a 10 cm long needle. The area inside the collar was then sprinkled with 300 mL DI water to wash the residual labeled solution on the litter into the soil. Subsequently, the collars were covered with the chambers, and a 50 mL gas sample was taken from the headspace with a gas-tight syringe at the time points of 4, 7, 24 and 30 h after the ^{15}N tracer injection. The gas samples (50 mL) were transferred into the Tedlar gas bags (100 mL). At the end of incubation, five soil cores (0–20 cm) in each chamber were collected with a stainless steel sampler (2.5 cm diameter, 50 cm length) and composited to one sample. Field ambient air samples and composite soil samples (0–20 cm) were taken at the beginning of the incubations near each collar (within 15 cm distance).

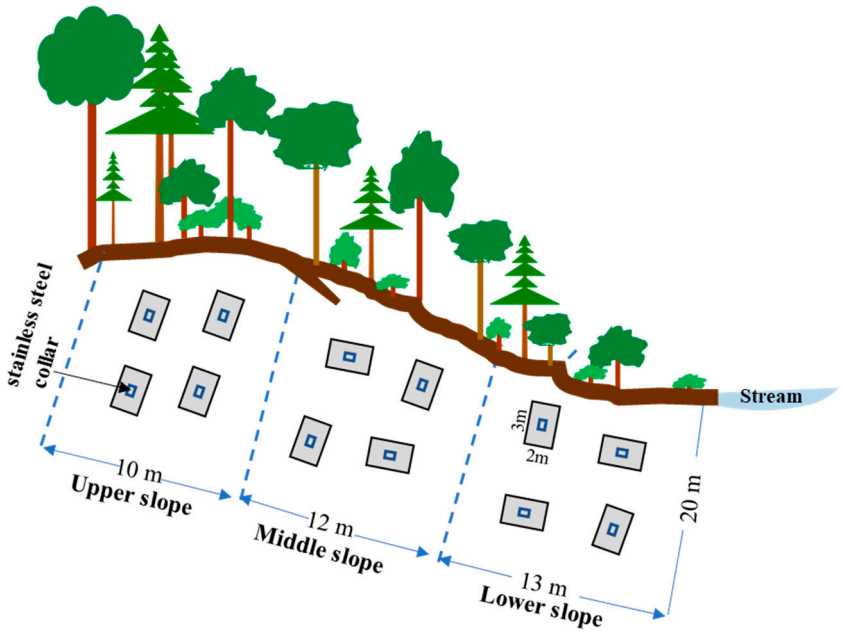

Figure 2. Schematic diagram of experimental design along slopes within each site (3 sites) selected in the mixed forest of Qingyuan station in Northeast China. In total, three slopes in each site were selected and used for gas emission measurements.

In June 2017, an additional two transects (site 2 and site 3, respectively), where the aspect, vegetation composition and soil texture were similar to those in site 1, were established in the same forest and divided into lower, middle, and upper slopes as three different soil moisture zones. Using the same procedures as mentioned above, four stainless steel collars on each slope of site 1, site 2, and site 3 were randomly inserted into the soil

one week before soil ^{15}N labeling, and the same dose of ^{15}N tracer solution was injected into the soil. The gas and soil samples were collected in the same way as described above.

2.3. Soil N_2O, N_2 Analysis and Flux Calculation

A 5 mL gas sample was injected into the gas chromatography for analyzing N_2O concentrations (C). The gas chromatography was fitted with a Porapak Q column (30 m length, 0.53 mm id) and equipped with an electron capture detector (ECD) (GC-2014, Shimadzu, Kyoto, Japan). Three standard N_2O samples with concentrations of 0.35, 5, 20 ppm (National Center for Standard Matters, Beijing, China) were used to calibrate the sample N_2O concentration. The bulk N_2O flux (F_{N_2O}, $\mu g \cdot m^{-2} \cdot h^{-1}$) was calculated from the linear change in N_2O concentration over time and the following Equation (1):

$$F_{N_2O} = (dC_T/dT) \times \rho_{N_2O} \times V/A \quad (1)$$

where bulk N_2O flux includes the fluxes from ^{15}N-labeled and non-labeled sources; C_T is the N_2O concentration in the mixed gases at the incubation time T (ppm); ρ_{N_2O} is the N_2O density at an air temperature of 20 °C in the field; V and A are the volume (m^3) and basal area (m^2) of the chamber.

The enrichment of ^{15}N in N_2O was measured by an IsoPrime trace gas analyzer (TG) coupled with an auto-sampler of 112 plots (Gilson GX-271, Dunstable, UK) and a continuous-flow isotope ratio mass spectrometer (IRMS, IsoPrime 100, Cheadle, UK). The peak areas for major ($^{44}N_2O$), minor 1 ($^{45}N_2O$), and minor 2 ($^{46}N_2O$) from IRMS, as well as the ratios ^{45}R ($^{45}N_2O/^{44}N_2O$) and ^{46}R ($^{46}N_2O/^{44}N_2O$), were reported in all the gas samples from enriched (Tm = 4, 7, 24, 30 h) and ambient air samples ($T0$). Previous studies showed that the non-random ^{15}N distribution in N_2O was observed due to the high ^{15}N enrichment in the source pool [8]. Hence, the ^{15}N enrichment of N_2O ($^{15}X_{N_2O}$) at each time point was calculated according to the ratios of ^{45}R and ^{46}R with the following Equation (2), assuming ^{17}R ($^{17}O/^{16}O$) = 3.8861 × 10^{-4} and ^{18}R ($^{18}O/^{16}O$) = 2.0947 × 10^{-3} [8,39]. The $^{15}N_2O$ flux ($F^{15}N_2O$) was estimated through bulk N_2O flux and the ^{15}N difference of N_2O enrichment between enriched and air samples. Furthermore, the N_2O flux produced from denitrification ($F_{N_2O_{denitrification}}$) was calculated by dividing the $^{15}N_2O$ flux by ^{15}N enrichment of the soil-labeled NO_3^- pool ($^{15}X_{NO_3^-}$) [8,40].

$$^{15}X_{N_2O} = 100 \times \frac{^{45}R + 2 \times {}^{46}R - {}^{17}R - 2 \times {}^{18}R)}{2 + 2 \times {}^{45}R + 2 \times {}^{46}R} \quad (2)$$

$$F^{15}N_2O = (^{15}X_{N_2O-Tm} - {}^{15}X_{N_2O-T0})/100 \times F_{N_2O} \quad (3)$$

$$F_{N_2O_{denitrification}} = F^{15}N_2O/{}^{15}X_{NO_3^-} \quad (4)$$

The content and rate of N_2 in samples were also determined using the TG-IRMS system. Gas sample (0.5 mL) was manually injected into the sample loop (50 µL) using a gas-tight syringe and the peak areas for major ($^{28}N_2$), minor 1 ($^{29}N_2$), and minor 2 ($^{30}N_2$) from IRMS as well as the ratios ^{29}R ($^{29}N_2/^{28}N_2$) and ^{30}R ($^{30}N_2/^{28}N_2$) were measured in both enriched (Tm = 4, 7, 24, 30 h) and ambient air samples ($T0$). According to the difference in the ratios ^{29}R and ^{30}R, respectively, between the sample and normal air, the ^{15}N mole fraction ($^{15}X_{N_2}$) and ^{15}N flux ($F^{15}N_2$) of N_2 at each time point were calculated using the following Equations (5) and (6). Then, the N_2 flux produced from denitrification ($F_{N_2denitrification}$) at each time point was calculated using Equation (7) by dividing the $^{15}N_2$ flux by ^{15}N enrichment of soil NO_3^- pool. The total N_2 flux ($F_{N_2-total}$) was estimated by dividing ^{15}N flux by the ^{15}N enrichment of N_2O pool ($^{15}X_{N_2O}$), assuming that N_2 production is from both denitrification-derived N_2O and NH_4^+ oxidation-derived N_2O [8].

$$^{15}X_{N_2} = \frac{^{29}R + 2 \times {}^{30}R}{2 + 2 \times {}^{29}R + 2 \times {}^{30}R} \quad (5)$$

$$F^{15}N_2 = \left({}^{15}X_{N_2-Tm} - {}^{15}X_{N_2-T0}\right) \times p_{N_2} \times V/(A \times T) \quad (6)$$

$$F_{N_2 denitrification} = F^{15}N_2/{}^{15}X_{NO_3^-} \quad (7)$$

$$F_{N_2-total} = F^{15}N_2/{}^{15}X_{N_2O} \quad (8)$$

where p_{N_2} is the density of N_2 at air temperature of 20 °C in the field; V and A are the volume (m^3) and basal area (m^2) of the chamber.

We did not directly measure the ^{15}N abundance of soil NO_3^- pool in this study. However, it can be calculated based on the ratios of ^{45}R and ^{46}R in N_2O, assuming that there is the same uniformly ^{15}N-labeled pool of NO_3^- for $^{15}N_2O$ and $^{15}N_2$ [41]. The detailed calculations can be found in Buchen et al. [40] and Spott et al. [42]. We further calculated $N_2O/(N_2O + N_2)$ ratios from denitrification (R_{N_2O}) according to $N_2O_{denitrification}$ and $N_{2denitrification}$ fluxes. The denitrification rates were present by the sum of $N_2O_{denitrification}$ plus $N_{2denitrification}$ fluxes. The total $N_2O/(N_2O + N_2)$ ratios ($R_{N_2O\text{-}total}$) were also calculated by total N_2 and bulk N_2O fluxes.

In this study, we defined three times the standard deviation as the minimum detectable change for N_2 and N_2O measurements [8]. Ultrahigh-purity N_2 gas (−1.63‰ $\delta^{15}N$) was manually injected (n = 60), and N_2O standard gas (0.37 ppm, n = 30) was automatically injected, in every batch as quality controls. The detection limit was 4.6×10^{-7} for ^{29}R, 3.9×10^{-7} for ^{30}R, 0.11‰ for $\delta^{15}N$ or 4×10^{-5} atom% ^{15}N in N_2, and 7.8×10^{-6} for ^{45}R, 3.8×10^{-5} for ^{46}R in N_2O. These values were applied to determine if the sample at each time point was significantly different from reference samples (T = 0 h), and if not, they were defined as having no ^{15}N-N_2 or N_2O production at this time point.

2.4. Soil Parameter Analysis

The soil samples were analyzed for bulk density (BD), soil moisture, pH, total nitrogen (TN), total organic carbon (TOC), and inorganic nitrogen (NH_4^+, NO_3^-) contents. Soil NH_4^+ and NO_3^- were extracted with 2 M KCl and measured by an auto discrete analyzer (Smartchem 200, Rome, Italy). The soil pH was determined by a pH meter (PHS-3E, INESA Scientific Instrument Co., Ltd., Shanghai, China) in a 1:2.5 soil water suspension. The TN and TOC contents were determined using an elemental analyzer (Micro Isotope Cube, Langenselbold, Germany). Soil BD was measured using a known volume metal container. Soil gravity water content (SGWC) was quantified by drying in oven at 105 °C for 24 h to a constant weight. The corresponding soil water-filled pore space (WFPS) was calculated based on BD and SGWC ($WFPS = \frac{SGWC \times BD}{1 - BD/2.65} \times 100\%$). The main soil characteristics were shown in Table 1.

2.5. Statistical Analyses

Prior to statistical analysis, data were checked for normality and homogeneity of variance with the Kolmogorov–Smirnov test and Levene's test, respectively. All statistical analyses were performed with SPSS software (Version 16.0; SPSS Inc., Chicago, IL, USA). One-way ANOVA was used to check the differences in rates of N_2 and N_2O emissions, $N_2O/(N_2O + N_2)$ ratios, and soil properties among slopes followed by multiple comparisons using the LSD method. Paired-samples t-test was applied to determine the differences in soil moisture, NH_4^+, and NO_3^- contents between before and after ^{15}N labeled incubation. The relationships between rates and ratios of gaseous N emissions and soil properties were examined using Pearson correlation analysis and regression analysis. To identify the dominant factors regulating soil N_2 and N_2O emissions as well as $N_2O/(N_2O + N_2)$ ratios, a stepwise regression analysis was conducted. The statistically significant differences were set at a 0.05 level unless otherwise stated.

3. Results

3.1. Soil Physical-Chemical Parameters

The soil water-filled pore space (WFPS) varied from 28% to 128% and was distinctly different among slopes, with higher values at the lower slope (Table 1). In contrast, soil pH had no significant variation among slopes, except site 1 in 2015. The total average soil BD increased from the lower (0.47 ± 0.03 g cm^{-3}) to the upper slope (0.59 ± 0.02 g cm^{-3}). Higher average contents of TOC, TN, NH_4^+ and ratios of C/N, NH_4^+/NO_3^- were observed at the lower slope. The total average NO_3^- contents were significantly higher at the upper and middle slopes than at the lower slope, although there were no significant differences among slopes within sites (Table 1). After soil ^{15}N was labeled for 30 h, no significant differences were found in soil moisture and NH_4^+ content, except NO_3^- content (Figure S2).

3.2. Soil N_2O and N_2 Emissions

Soil bulk N_2O emissions (except site 1 in 2015) peaked at 7 h and then decreased with incubation time (Figure 3A). The average bulk N_2O emission rates from 7 to 30 h decreased more at the upper slope (62%) than the lower and middle slope (8% and 15%, respectively). However, the $^{15}N_2O$ emissions at the upper slope did not follow the same pattern as bulk N_2O emissions (Figure 3B). Over the 30 h incubation, the mean bulk N_2O fluxes varied significantly across slopes, with higher values at the lower slope (Figure 4A, Table 2). A similar pattern was also observed in the denitrification-derived N_2O fluxes (Figure 4B).

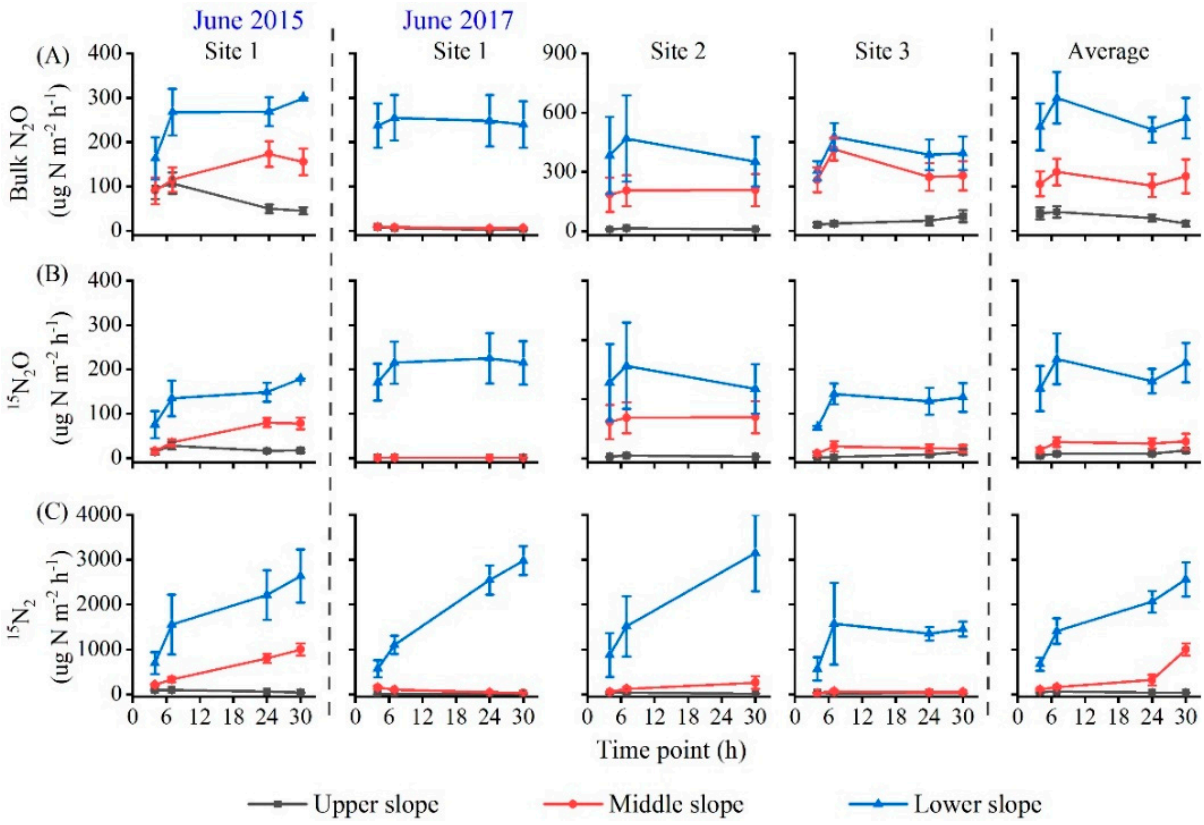

Figure 3. Emission rates of soil bulk N_2O (**A**), $^{15}N_2O$ (**B**) and $^{15}N_2$ (**C**) with incubation time after in situ $^{15}NO_3^-$ addition (2.5 g ^{15}N m^{-2}) at different slope positions in the mixed forest of Qingyuan station in Northeast China. Values from different sites (1, 2, 3) and the overall average are shown.

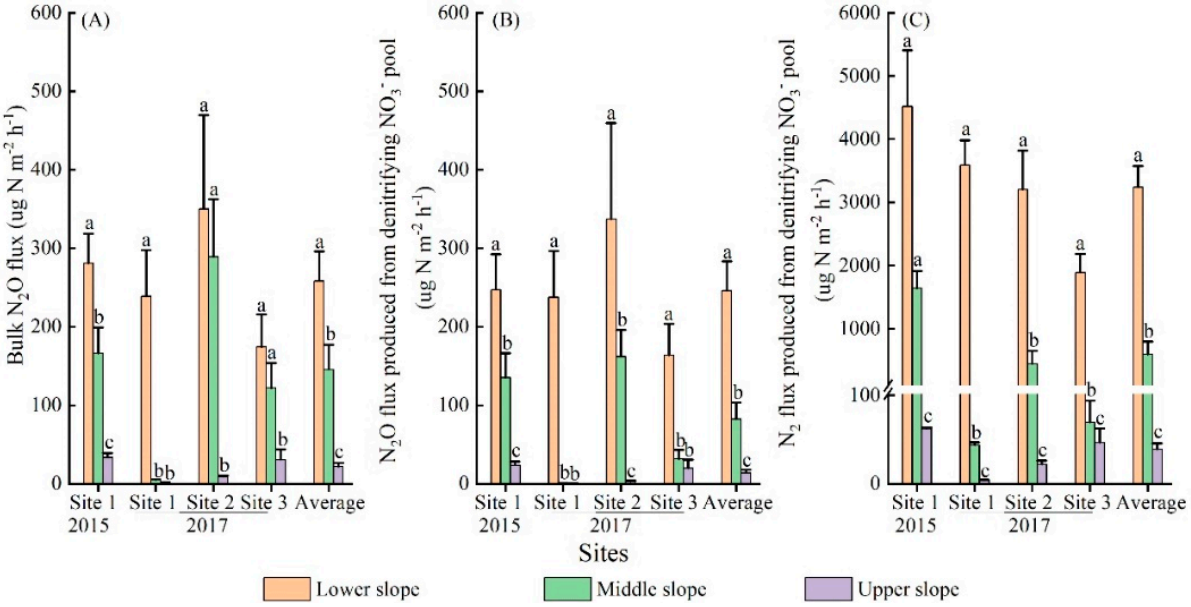

Figure 4. Mean fluxes of bulk N_2O (**A**), N_2O (**B**) and N_2 (**C**) produced from denitrifying NO_3^- pool over a 30 h incubation after in situ $^{15}NO_3^-$ addition (2.5 g ^{15}N m^{-2}) at different slope positions in the mixed forest of Qingyuan station in Northeast China. Values from different sites (1, 2, 3) and overall average are shown. Different lowercase letters indicate significant differences among slopes ($p < 0.05$).

Table 2. The area-weighed N_2 and N_2O fluxes and ratios in the mixed forest of Qingyuan station in Northeast China.

Slope Positions	Area (%)	$N_2O_{denitrification}$ (μg N m^{-2} h^{-1})	Bulk N_2O (μg N m^{-2} h^{-1})	$N_{2denitrification}$ (μg N m^{-2} h^{-1})	Total N_2 (μg N m^{-2} h^{-1})	Denitrification (μg N m^{-2} h^{-1})	R_{N_2O}	$R_{N_2O\text{-total}}$
Upper	80	14 ± 4 c	22 ± 5 c	39 ± 7 c	85 ± 15 c	54 ± 10 c	0.22 ± 0.03 a	0.20 ± 0.02 a
Middle	15	82 ± 21 b	145 ± 32 b	594 ± 205 b	896 ± 243 b	676 ± 220 b	0.20 ± 0.05 a	0.18 ± 0.04 a
Lower	5	246 ± 38 a	258 ± 37 a	3243 ± 330 a	3442 ± 342 a	3488 ± 340 a	0.08 ± 0.01 b	0.08 ± 0.01 b
Total	100	36 ± 8	52 ± 11	282 ± 53	375 ± 66	319 ± 58	0.16 ± 0.02	0.15 ± 0.02

Different lowercase letters indicate significant differences among slopes ($p < 0.05$). Denitrification: the sum of $N_2O_{denitrification}$ plus $N_{2denitrification}$; R_{N_2O}: ratio of $N_2O_{denitrification}$ to $N_2O_{denitrification}$ plus $N_{2denitrification}$; $R_{N_2O\text{-total}}$: ratio of bulk N_2O to bulk N_2O plus total N_2.

Similar to $^{15}N_2O$, the $^{15}N_2$ emissions with incubation time at each slope position also had different patterns among sites (Figure 3C). The average $^{15}N_2$ emissions at the lower and middle slopes significantly increased with incubation time, while a slight downward trend was observed at the upper slope (Figure 3C). Furthermore, the N_2 flux produced from denitrifying NO_3^- pool ($N_{2denitrification}$) varied from 4 to 4517 μg N m^{-2} h^{-1} among sites, being much higher than N_2O emissions (Figure 4). A large variation in denitrification rate (N_2 + N_2O) was also observed among sites (Figure S3A). Overall, the mean fluxes of $N_{2denitrification}$ and total N_2, as well as denitrification rates, significantly decreased from the lower to the upper slope (Table 2, Figures 4C and S3A).

3.3. Soil $N_2O/(N_2O + N_2)$ Ratio

Significant variations in R_{N_2O} (ratio of $N_2O_{denitrification}$ to $N_2O_{denitrification}$ plus $N_{2denitrification}$) among slopes were observed in all sites (Figure S3B). This ratio at the lower slope was significantly lower than those at the middle and upper slopes (Table 2). Based on the areas of different soil moisture zones occupied in the study forest, the weighted average R_{N_2O} was 0.16 ± 0.02, being similar to $R_{N_2O\text{-total}}$ (ratio of bulk N_2O to bulk N_2O plus total N_2, 0.15 ± 0.02) (Table 2). Further, the area-weighted R_{N_2O} and $R_{N_2O\text{-total}}$ were much lower than the value of soil $N_2O/(N_2O + N_2)$ ratio (0.30) from natural forests recompiled by those previously reported literature (Table S1).

3.4. Relationships between Gaseous N Rates, Ratios, and Soil Properties

Soil N_2, $N_2O_{denitrification}$, bulk N_2O and denitrification rates were all positively correlated with soil WFPS, TOC, C/N and NH_4^+/NO_3^- ratio, while they had a negative correlation with BD (Table 3). The R_{N_2O} was negatively correlated with soil WFPS and C/N ratio (Table 3). A stepwise regression analysis showed that soil WFPS was the key factor regulating $N_{2denitrification}$, denitrification rate and R_{N_2O}, accounting for 63%, 63% and 13% of variation, respectively (Table 4). In contrast, the C/N and NH_4^+/NO_3^- ratios mainly affected the emissions of bulk N_2O and $N_2O_{denitrification}$ (Table 4).

Table 3. Pearson correlations between soil properties and fluxes, ratios of N_2 and N_2O emissions in the mixed forest of Qingyuan station in Northeast China.

	$N_{2denitrifcation}$	$N_2O_{denitrifcation}$	Denitrification	R_{N_2O}	$R_{N_2O\text{-}total}$	Bulk N_2O	Total N_2
BD	−0.36 *	−0.34 *	−0.37 *	0.19	0.26	−0.38 *	−0.37 *
pH	−0.24	0.05	−0.22	0.20	0.27	0.10	−0.23
WFPS	0.74 **	0.51 **	0.73 **	−0.39 **	−0.41 **	0.47 **	0.75 **
TOC	0.45 **	0.38 *	0.46 **	−0.16	−0.18	0.42 **	0.45 **
TN	0.29	0.24	0.29	−0.12	−0.14	0.28	0.28
C/N ratio	0.62 **	0.54 **	0.63 **	−0.35 *	−0.39 *	0.52 **	0.63 **
NH_4^+	0.23	0.19	0.23	0.01	0.05	0.28	0.22
NO_3^-	−0.21	−0.18	−0.21	0.11	0.03	−0.17	−0.19
NH_4^+/NO_3^- ratio	0.31 *	0.43 **	0.33 *	−0.06	0.01	0.46 **	0.30 *

* and ** represent correlation significance at $p < 0.05$ and $p < 0.01$, respectively.

Table 4. Multiple linear regression models between fluxes, ratios of N_2 and N_2O from denitrification, bulk N_2O flux and selected soil properties in the mixed forest of Qingyuan station in Northeast China.

Species	WFPS	BD	C/N Ratio	NH_4^+/NO_3^- Ratio	R^2
$N_{2denitrification}$	0.72 **	−0.32 **			0.63
$N_2O_{denitrification}$			0.48 **	0.35 **	0.38
Denitrification	0.71 **	−0.33 **			0.63
R_{N_2O}	−0.38 *				0.13
Bulk N_2O			0.45 **	0.38 **	0.38

* and ** represent significance at $p < 0.05$ and $p < 0.01$, respectively. R square represents the determination coefficient.

4. Discussion

4.1. Variations of Soil N_2 and N_2O Emissions

The ^{15}N isotope tracer technique allows us to determine in situ N_2 as well as N_2O emissions due to denitrification. In our study, soil N_2 emissions were mainly produced by denitrification (area-weighted: 282 μg N m^{-2} h^{-1}) and denitrification accounted for average 75% of total N_2 emissions (area-weighted: 375 μg N m^{-2} h^{-1}, Table 2), which was consistent with our previous laboratory findings at the same study site [37]. The mean N_2 fluxes compared well with the rates reported from a woodland forest in the UK [28], a forested wetland and a northern hardwood forest in the US [7,27], using the similar ^{15}N tracer approach. Our result was also comparable to the rates reported in other temperate forests and maize soils using the gas–flow soil core method [11,13]. Furthermore, the fluxes of both bulk N_2O and $N_2O_{denitrification}$ were significantly lower in comparison with the N_2 fluxes (Table 2, Figures 3 and 4), which was consistent with the results reported from the ^{15}N tracer studies in temperate forests [27], tropical forests [8,30], and other upland soils [43]. Therefore, our results, together with those of previous studies, suggest that N_2 emissions are likely the main gaseous N loss from terrestrial ecosystems. Moreover, the total denitrification rate ($N_2 + N_2O$) (54 to 3488 μg N m^{-2} h^{-1}, Table 2) was in the range reported in the laboratory ^{15}N tracer assay [7]. In contrast, this rate was significantly higher than those in other temperate forests from in situ ^{15}N tracer studies [27,28]. This may be partly explained by the differences in NO_3^- and water input. In previous studies, the added

NO_3^- and water only adjusted within 10% and 5% of the ambient soil NO_3^- pool and volumetric water, respectively. In our study, however, soil–extracted NO_3^- significantly increased by more than 5 times (Figure S2C). Moreover, about 11 mm precipitation was deposited into the soil, potentially leading to a 10% increase in soil volumetric, although no significant change was observed in soil gravity water content (Figure S2A). One laboratory ^{15}N study from a tropical rainforest showed an increase in N_2O emission with increasing soil NO_3^- [8]. Additionally, high water input to soil may promote the formation of an anaerobic environment, potentially promoting the further reduction of the produced N_2O to N_2 during denitrification [30]. The significantly higher N_2 rather than N_2O flux from denitrification, was confirmed in our study (Table 2, Figures 3 and 4).

In this study, we found the highest N_2 and N_2O emissions or denitrification rates occurring at the lower slope (Table 2, Figures 4 and S3A). This was partly in line with our expectations. Topography plays an important role in the redistribution of water and substrates (available N or C) which can influence gaseous N emissions [17]. Substrates are prone to accumulate in the bottom position with the transportation of water [31,44]. In the present study, the lower slope had higher soil WFPS, TOC, TN, NH_4^+ contents and lower soil BD compared to the upper slope, and the variation in soil WFPS across slopes was significantly larger than other soil parameters (Table 1). Previous studies indicated that soil water could affect the production of N gas from nitrification and denitrification by regulating O_2 and/or substrate availability [31,45]. In this study, we found that soil WFPS was significantly positively correlated with TOC and C/N ratio (Table S2). Furthermore, good positive relationships between soil WFPS and $N_{2denitrification}$ flux, denitrification rate were observed, although soil BD had a negative contribution to denitrification rate and $N_{2denitrification}$ flux (Table 4). It suggests that the change in soil water associated with bulk density is important factor driving the difference in denitrification across slopes. Additionally, it was noted that the underestimated N_2O and N_2 fluxes may occur in the current study due to the gas diffusion from soil surface to subsoil. Previous study demonstrated a large underestimation of denitrification rate from the soil surface using static chamber method and the underestimated extent could decrease with the increase in soil moisture [46]. In the present study, we speculated that the N_2 and N_2O fluxes measured at the lower slope were likely to reflect real values since soil water was oversaturated in this location (110% WFPS). However, these fluxes will be significantly underestimated at the middle and upper slopes, where soil WFPS were 40% and 60%, respectively, slightly lowering the values reported by Well et al. [46]. Nevertheless, our field results are consistent with previous laboratory findings, where high soil moisture corresponded to high N_2 and N_2O emissions [7,9]. These results confirm that the change in soil moisture could moderate the variations of N_2 and N_2O emissions.

In addition to soil moisture, the relative proportion of N_2 and N_2O was affected by N substrates [7,8]. The N availability, such as NO_3^- and NH_4^+, is the primary requirement for denitrification and nitrification [17]. The high nitrification rates and NO_3^- contents were reported at lower slope sites in a temperate coniferous forest [44]. Previous assays indicated the simultaneous increase in N_2 and N_2O production with the increase in NO_3^- concentration [8,12]. However, our study showed a high NO_3^- content at the middle and upper slopes, which did not have the highest gaseous N emissions (Table 1, Figure 4). Alternatively, we found that soil N_2O emissions were affected by the NH_4^+/NO_3^- ratio (Tables 3 and 4), which was inconsistent with previous findings. It was likely that the relative proportion of substrate N species in comparison to their contents may be more important to N_2O rather than N_2 emissions. Moreover, the C/N ratio significantly affected soil bulk N_2O and $N_2O_{denitrification}$ fluxes (Table 4), although soil TOC, C/N, or bulk density was individually observed to correlate with these fluxes (Table 3). These relationships indicate that the changes in soil parameters may have the different effects on N_2 and N_2O emissions. In addition, the temporal variation in N_2O and N_2 emissions was larger at the upper and middle slopes within the site (Figure 4). This suggests that the in situ

denitrification rates may change with the seasons or years [28]. Therefore, the dynamics of in situ soil N_2 and N_2O fluxes should be addressed in the future.

4.2. Comparison of Soil $N_2O/(N_2O + N_2)$ Ratios from Denitrification

Spatial variations of N_2 and N_2O emissions in this study were expected. Commonly measured N_2O fluxes are widely available, yet to accurately estimate denitrification rates requires a better understanding of the controls on $N_2O/(N_2O + N_2)$ ratios from denitrification (R_{N_2O}). In the current study, lower R_{N_2O} were associated with high soil moisture (Table 2, Figure S3B). Similar findings were also observed from other temperate forests in laboratory assays using ^{15}N labeling [7] or the direct gas flux method [11]. Increasing soil moisture will decrease O_2 diffusion, most likely forming anaerobic conditions for denitrification, and it is expected that the R_{N_2O} will decrease [47]. Besides, NO_3^- availability, as the electron acceptor of denitrification, also affected its product ratio [13]. However, our results demonstrated that this ratio was mainly regulated by soil moisture (Table 4), further supporting our previous hypothesis. Moreover, the area-weighted average R_{N_2O} from the entire forest (0.16, Table 2) was similar to the value from the ^{15}N gas flux method reviewed by Scheer et al. [24]. In contrast, our result was significantly lower than previously reviewed global ratios in upland soils based on approaches of ^{15}N trace and acetylene inhibition [16], while it was higher compared to previous field ^{15}N trace studies on temperate forests (e.g., 0.008 and 0.01 in Refs. [27,28], respectively). We further calculated the R_{N_2O} from forest soils, with an average value of 0.30 (Table S1), by compiling these data from previous research [16,24] and our study. This reflected the great spatial variability of R_{N_2O}, and its dynamic change urgently requires to be clarified. Nevertheless, these results suggest that N_2 fluxes from forest ecosystems are likely to be underestimated by around one-third when using the $N_2O/(N_2O + N_2)$ ratio in nature soils reported by Schlesinger [16].

Previous studies indicated the variations in the $N_2O/(N_2O + N_2)$ ratio due to the difference in N_2 measurement among methods [41]. Based on the literature compiled with the current study, we observed a significant difference in $N_2O/(N_2O + N_2)$ ratios among methods, with the highest values observed by the acetylene inhibition method and the lowest values by the ^{15}N tracer method (Figure S4). As reported in previous studies, each method has a special application range and its advantage or disadvantage [11,48]. For instance, the ^{15}N-gas flux method requires reasonable amounts of labeled NO_3^- introduced to soil systems, which may disturb the soil micro−environment and stimulate microbial N turnover [11], affecting soil N_2 emission. Therefore, the approach used in this study also had some bias for N_2 measurement. These bias may be linked to the amount of added NO_3^- and water, labeled soil depth, enclosure time and volume of the chamber, and even the precision of the instrument [8,41,46,48]. In our study, soil NO_3^- and moisture were higher than the common conditions (Figure S2A,C), although a high NO_3^- content (i.e., >20 mg N kg^{-1}) was often observed in some natural temperate forests in the same region as our study [49]. As discussed above, the potential interaction of NO_3^- and water regulated the proportion of N_2 and N_2O emissions, leading to a lower $N_2O/(N_2O + N_2)$ ratio than the real ratios. As a result, it was likely to overestimate N_2 emission and underestimate R_{N_2O}. In the preliminary experiment, we did not find a significant change in the $\delta^{15}N$-N_2 value between the labeled sample (24 h) and ambient air (0 h) after the soil was labeled with $^{15}NO_3^-$ solution at a rate of 0.25 g ^{15}N m^{-2} (data not shown). Furthermore, an unknown proportion of downward diffusion of ^{15}N−labeled gases to the non−labeled subsoil might cause the bias in N_2 and N_2O fluxes [41,46]. The extend closure time of chamber would further add the variations. Although the fluxes of $^{15}N_2$ and $^{15}N_2O$ at all the slopes were found to increase during 30 h incubation (Figure 3B,C), the ^{15}N gas diffusion to the subsoil (below 10 cm) could occur, especially on the middle and upper slopes with larger air-filled porosity (Table 1). Moreover, the large volume of the chamber (18 L) likely diluted the produced $^{15}N_2$ with air ^{14}N. Consequently, it could lead to an underestimation of N_2 fluxes. These were thus responsible for the observation of low or undetectable N_2 flux explained in part due to these effects (Figure S5). In addition, quantifying the limit of

detection for the ^{15}N gas flux method is still a challenge in low N_2 emissions in nature forest ecosystems, although the detection sensitivity of our IRMS (0.79 μg ^{15}N m^{-2} h^{-1}) is better compared to previous studies [8,27,28]. As addressed above, undoubtedly, there are still some other bias regarding the accuracy of N_2 loss due to the interactions of multiple and unpredictable factors. Therefore, some improvements could be explored to reduce these bias for the in situ ^{15}N tracer method. For example, one way to improve detection is to reduce the N_2 background concentration in the field by flushing chambers with a N_2–free air [20]. Additionally, based on this, shorting chamber height and sampling time can further improve the N_2 analytical accuracy. Overall, more field studies on N_2 emissions and the $N_2O/(N_2O + N_2)$ ratios from forest ecosystems with ^{15}N tracer method are required in the future.

4.3. Implications for Ecosystem N Loss

In this study, about 5.1 kg N ha^{-1} yr^{-1} of total N_2 flux was estimated based on the area–weighted total $N_2O/(N_2O + N_2)$ ratio (0.15, Table 2) and the field average N_2O flux with 0.90 kg N ha^{-1} yr^{-1} monitored in 2019 to 2021 (Huang K. et al., unpublished). The actual N_2 fluxes were probably higher than this estimate because the chambers for monitoring field N_2O flux were mostly set at the upper and middle slope positions, where N_2O emissions were relatively lower than those at the lower slope position (Table 2). The total gaseous N emissions ($N_2 + N_2O$) were calculated at about 6.0 kg N ha^{-1} yr^{-1}, accounting for 30% of the inorganic N (NH_4^+ plus NO_3^-, 20 kg N ha^{-1} yr^{-1}) deposition in precipitation, as reported in this study forest by Huang et al. [35]. This result was comparable to those from Hawaiian rainforests [50,51] and temperate forests [52] estimated by the natural nitrogen and/or oxygen stable isotope approach. In all, these findings suggest that the gaseous N losses from the forest ecosystems may be larger than commonly thought, and the N cycle is likely to be more open.

The present study still have some uncertainties in estimating soil N_2 flux with measured $N_2O/(N_2O + N_2)$ ratio, including the bias from the ^{15}N–gas flux method as mentioned above. For instance, previous studies indicated the variations in $N_2O/(N_2O + N_2)$ ratios during different growing periods [26,28]. In the current study, we carried out the ^{15}N trace experiment in the middle period of the growing season (April to October) and monitored the N gas emission once. In this period, soil temperature was high which stimulated microbial activity to consume considerable substrates for nitrification and denitrification. These processes in turn promoted gaseous N losses from soil. In the early or later phase, however, plant growth and microbial activities may decrease due to temperature limitations. Low available substrates could affect microbial enzyme activity and community composition, causing an increase or decrease in $N_2O/(N_2O + N_2)$ ratios [17]. As a result, the calculated N_2 loss was under– or over–estimated. Moreover, the change in soil moisture could affect the diffusion of N_2 and N_2O produced in soil pore space [41], leading to the differences in the $N_2O/(N_2O + N_2)$ ratios among different periods. It was found that field soil WFPS changed from 24% to 73% throughout the growing season in our study site [34]. Previous studies showed a low $N_2O/(N_2O + N_2)$ ratio with high soil moisture [7,15], being similar to our result. The effect extent of soil moisture on $N_2O/(N_2O + N_2)$ ratio remains unclear and should be further clarified in the following studies. Additionally, the unquantified other microbial processes from N_2 and N_2O emissions are also contributed to the uncertainty in $N_2O/(N_2O + N_2)$ ratios. More field research on differentiating production pathways of N_2 and N_2O emissions from forest ecosystems are urgently required for more robust estimates of gaseous N losses [53].

5. Conclusions

The results of this study showed that in situ soil N_2 and N_2O emissions significantly varied across slopes and were strongly affected by soil moisture. Soil N_2 emissions were significantly higher compared to N_2O emissions, accounting for 85% of gaseous N losses ($N_2 + N_2O$). The combined field N_2O flux and $N_2O/(N_2O + N_2)$ ratio is likely to be a

promising tool to quantify soil N_2 flux and even denitrification rate for a given forest ecosystem. In addition, we recognize that there are some bias for determining in situ soil N_2 emission and therefore the calculated $N_2O/(N_2O + N_2)$ ratio in the current ^{15}N trace study, such as the added $^{15}NO_3^-$ amount, enclosure time of the chamber, and gas diffusion to the subsoil. Overall, to further elucidate the dynamic of soil N_2 and N_2O emissions associated with $N_2O/(N_2O + N_2)$ ratios, in situ ^{15}N–labeled experiments in different seasons from different forest ecosystems should be performed. Meanwhile, we also need to refine and combine established methodologies using models for better predicting ecosystem denitrification rate and gaseous N losses.

Supplementary Materials: The following supporting information can be downloaded at: https://www.mdpi.com/article/10.3390/f13091347/s1, Figure S1: The sampling photos at the three slope positions in site 1 in the mixed forest of Qingyuan station in Northeast China; Figure S2: Changes of 0–20 cm in soil moisture (A, express as gravity water content), ammonium (NH_4^+, B), and nitrate (NO_3^-, C) contents before and after ^{15}N labeling at different slope positions in the mixed forest of Qingyuan station in Northeast China. Differences were analyzed by paired-samples *t*-test ($p < 0.05$); Figure S3: The rates (A) and $N_2O(N_2O + N_2)$ ratios (B) from denitrification over a 30 h incubation after in situ $^{15}NO_3^-$ addition (2.5 g ^{15}N m^{-2}) at different slope positions in the mixed forest of Qingyuan station in Northeast China. Values from different sites (1, 2, 3) and overall average were shown. Different lowercase letters indicate significant differences among slopes ($p < 0.05$); Figure S4. Comparison of $N_2O/(N_2O + N_2)$ ratios obtained by different methods for forest soils. Figure S5: Changes of $\delta^{15}N$-N_2 (‰) value with incubation time at the lower (A), middle (B), and upper (C) slope in site 1, respectively, after soil was labeled with NO_3^- addition (2.5 g ^{15}N m^{-2}) in the mixed forest of Qingyuan station in Northeast China. The red dotted line indicates the minimum detectable change for $\delta^{15}N$ (0.11‰) and the error bars represent standard errors; Table S1: Recompilation of the values of $N_2O/(N_2 + N_2O)$ ratio in natural forest soils; Table S2: Pearson correlation between soil properties in the mixed forest of Qingyuan station in Northeast China.

Author Contributions: Conceptualization, Y.F. and W.Z.; Investigation, D.X.; Writing—original draft, D.X.; Writing—review and editing, Y.F. and W.Z. All authors have read and agreed to the published version of the manuscript.

Funding: This research was financially supported by the National Key Research and Development Program of China (Grant Nos. 2016YFA0600802, 2017YFC0212704-01), the National Natural Science Foundation of China (Grant Nos. 41703068, 41773094), the Key Research Program of Frontier Sciences of Chinese Academy of Sciences (Grant No. QYZDB-SSW-DQC002), Research and Development Project of Scientific Instruments and Equipment of Chinese academy of sciences (Grant No. YJKYYQ20190054), and the Project of Forestry Peak Discipline at Fujian Agriculture and Forestry University, China (Grant No. 118—71201800724).

Data Availability Statement: Data are contained within the article or Supplementary Materials.

Acknowledgments: We greatly thank Shasha Zhang, Shanlong Li, Xiaoming Fang, Shaonan Huang, for their help on the field gas sampling, Feifei Zhu, Dongwei Liu, and Kai Huang for suggestions on data analysis and the presentation of results of the study.

Conflicts of Interest: The authors declare no conflict of interest.

References

1. Butterbach-Bahl, K.; Baggs, E.M.; Dannenmann, M.; Kiese, R.; Zechmeister-Boltenstern, S. Nitrous oxide emissions from soils: How well do we understand the processes and their controls? *Philos. Trans. R. Soc. B* **2013**, *368*, 20130122. [CrossRef] [PubMed]
2. Galloway, J.N.; Dentener, F.J.; Capone, D.G.; Boyer, E.W.; Howarth, R.W.; Seitzinger, S.P.; Asner, G.P.; Green, P.A.; Holland, E.A. Nitrogen cycles: Past, present, and future. *Biogeochemistry* **2004**, *70*, 153–226. [CrossRef]
3. Stange, C.F.; Spott, O.; Arriaga, H.; Menendez, S.; Estavillo, J.M.; Merino, P. Use of the inverse abundance approach to identify the sources of NO and N_2O release from Spanish forest soils under oxic and hypoxic conditions. *Soil Biol. Biochem.* **2013**, *57*, 451–458. [CrossRef]
4. Wallenstein, M.D.; Myrold, D.D.; Firestone, M.; Voytek, M. Environmental controls on denitrifying communities and denitrification rates: Insights from molecular methods. *Ecol. Appl.* **2006**, *16*, 2143–2152. [CrossRef]

5. Groffman, P.M.; Altabet, M.A.; Böhlke, J.K.; Butterbach-Bahl, K.; David, M.B.; Firestone, M.K.; Giblin, A.E.; Kana, T.M.; Nielsen, L.P.; Voytek, M.A. Methods for measuring denitrification: Diverse approaches to a difficult problem. *Ecol. Appl.* **2006**, *16*, 2091–2122. [CrossRef]
6. Yoshinari, T.; Hynes, R.; Knowles, R. Acetylene inhibition of nitrous oxide reduction and measurement of denitrification and nitrogen fixation in soil. *Soil Biol. Biochem.* **1977**, *9*, 177–183. [CrossRef]
7. Morse, J.L.; Bernhardt, E.S. Using ^{15}N tracers to estimate N_2O and N_2 emissions from nitrification and denitrification in coastal plain wetlands under contrasting land-uses. *Soil Biol. Biochem.* **2013**, *57*, 635–643. [CrossRef]
8. Yang, W.H.; McDowell, A.C.; Brooks, P.D.; Silver, W.L. New high precision approach for measuring ^{15}N-N_2 gas fluxes from terrestrial ecosystems. *Soil Biol. Biochem.* **2014**, *69*, 234–241. [CrossRef]
9. Morse, J.L.; Durán, J.; Groffman, P.M. Soil denitrification fluxes in a northern Hardwood forest: The importance of snowmelt and implications for ecosystem N budgets. *Ecosystems* **2015**, *18*, 520–532. [CrossRef]
10. Morse, J.L.; Durán, J.; Beall, F.; Enanga, E.M.; Creed, I.F.; Fernandez, I.; Groffman, P.M. Soil denitrification fluxes from three northeastern North American forests across a range of nitrogen deposition. *Oecologia* **2015**, *177*, 17–27. [CrossRef]
11. Butterbach-Bahl, K.; Willibald, G.; Papen, H. Soil core method for direct simultaneous determination of N_2 and N_2O emissions from forest soils. *Plant Soil* **2002**, *240*, 105–116. [CrossRef]
12. Wang, R.; Feng, Q.; Liao, T.T.; Zheng, X.H.; Butterbach-Bahl, K.; Zhang, W.; Jin, C.Y. Effects of nitrate concentration on the denitrification potential of a calcic cambisol and its fractions of N_2, N_2O and NO. *Plant Soil* **2013**, *363*, 175–189. [CrossRef]
13. Wang, R.; Pan, Z.L.; Zheng, X.H.; Ju, X.T.; Yao, Z.S.; Butterbach-Bahl, K.; Zhang, C.; Wei, H.H.; Huang, B.X. Using field-measured soil N_2O fluxes and laboratory scale parameterization of $N_2O/(N_2O + N_2)$ ratios to quantify field-scale soil N_2 emissions. *Soil Biol. Biochem.* **2020**, *148*, 107904. [CrossRef]
14. Boyer, E.W.; Alexander, R.B.; Parton, W.J.; Li, C.S.; Butterbach-Bahl, K.; Donner, S.D.; Skaggs, R.W.; Del Gross, S.J. Modeling denitrification in terrestrial and aquatic ecosystems at regional scales. *Ecol. Appl.* **2006**, *16*, 2123–2142. [CrossRef]
15. Weier, K.L.; Doran, J.W.; Power, J.F.; Walters, D.T. Denitrification and the dinitrogen/nitrous oxide ratio as affected by soil water; available carbon; and nitrate. *Soil Sci. Soc. Am. J.* **1993**, *57*, 66–72. [CrossRef]
16. Schlesinger, W.H. On the fate of anthropogenic nitrogen. *Proc. Natl. Acad. Sci. USA* **2009**, *106*, 203–208. [CrossRef]
17. Saggar, S.; Jha, N.; Deslippe, J.; Bolan, N.S.; Luo, J.; Giltrap, D.L.; Kim, D.G.; Zaman, M.; Tillman, R.W. Denitrification and N_2O:N_2 production in temperate grasslands: Processes; measurements; modelling and mitigating negative impacts. *Sci. Total Environ.* **2013**, *465*, 173–195. [CrossRef]
18. Kulkarni, M.V.; Groffman, P.M.; Yavitt, J.B.; Goodale, C.L. Complex controls of denitrification at ecosystem; landscape and regional scales in northern hardwood forests. *Ecol. Model.* **2015**, *298*, 39–52. [CrossRef]
19. Liptzin, D.; Silver, W.L. Spatial patterns in oxygen and redox sensitive biogeochemistry in tropical forest soils. *Ecosphere* **2015**, *6*, 211. [CrossRef]
20. Well, R.; Burkart, S.; Giesemann, A.; Grosz, B.; Koester, J.R.; Lewicka-Szczebak, D. Improvement of the ^{15}N gas flux method for in situ measurement of soil denitrification and its product stoichiometry. *Rapid Commun. Mass Spectrom.* **2019**, *33*, 437–448. [CrossRef]
21. Burgin, A.J.; Groffman, P.M. Soil O_2 controls denitrification rates and N_2O yield in a riparian wetland. *J. Geophys. Res.* **2012**, *117*, 1010. [CrossRef]
22. Lai, T.V.; Denton, M.D. N_2O and N_2 emissions from denitrification respond differently to temperature and nitrogen supply. *J. Soils Sediment* **2018**, *18*, 1548–1557. [CrossRef]
23. Senbayram, M.; Well, R.; Bol, R.; Chadwick, D.R.; Jones, D.L.; Wu, D. Interaction of straw amendment and soil NO_3^- content controls fungal denitrification and denitrification product stoichiometry in a sandy soil. *Soil Biol. Biochem.* **2018**, *126*, 204–212. [CrossRef]
24. Scheer, C.; Fuchs, K.; Pelster, D.E.; Butterbach-Bahl, K. Estimating global terrestrial denitrification from measured N_2O:$(N_2O + N_2)$ product ratios. *Curr. Opin. Env. Sust.* **2020**, *47*, 72–80. [CrossRef]
25. Mogge, B.; Kaiser, E.A.; Munch, J.C. Nitrous oxide emissions and denitrification N-losses from forest soils in the Bornhöved Lake region (Northern Germany). *Soil Biol. Biochem.* **1998**, *30*, 703–710. [CrossRef]
26. Bai, E.; Li, W.; Li, S.L.; Sun, J.F.; Peng, B.; Dai, W.W.; Jiang, P.; Han, S.J. Pulse increase of soil N_2O emission in response to N addition in a temperate forest on Mt Changbai; Northeast China. *PLoS ONE* **2014**, *9*, e102765.
27. Kulkarni, M.V.; Burgin, A.J.; Groffman, P.M.; Yavitt, J.B. Direct flux and ^{15}N tracer methods for measuring denitrification in forest soils. *Biogeochemistry* **2014**, *117*, 359–373. [CrossRef]
28. Sgouridis, F.; Ullah, S. Relative magnitude and controls of in situ N_2 and N_2O fluxes due to denitrification in natural and seminatural terrestrial ecosystems using ^{15}N tracers. *Environ. Sci. Technol.* **2015**, *49*, 14110–14119. [CrossRef]
29. Pan, Y.; Birdsey, R.A.; Fang, J.; Houghton, R.; Kauppi, P.E.; Kurz, W.A.; Phillips, O.L.; Shvidenko, A.; Lewis, S.L.; Canadell, J.G.A. A large and persistent carbon sink in the world's forests. *Science* **2011**, *333*, 988–993. [CrossRef]
30. Tang, W.G.; Chen, D.X.; Phillips, O.L.; Liu, X.; Zhou, Z.; Li, Y.D.; Xi, D.; Zhu, F.F.; Fang, J.Y.; Zhang, L.M.; et al. Effects of long-term increased N deposition on tropical montane forest soil N_2 and N_2O emissions. *Soil Biol. Biochem.* **2018**, *126*, 194–203. [CrossRef]
31. Friedl, J.; Scheer, C.; Rowlings, D.W.; McIntosh, H.V.; Strazzabosco, A.; Warner, D.I.; Grace, P.R. Denitrification losses from an intensively managed sub-tropical pasture–Impact of soil moisture on the partitioning of N_2 and N_2O emissions. *Soil Biol. Biochem.* **2016**, *92*, 58–66. [CrossRef]

32. Luo, J.; Tillman, R.W.; Ball, P.R. Nitrogen loss through denitrification in a soil under pasture in New Zealand. *Soil Biol. Biochem.* **2000**, *32*, 497–509. [CrossRef]
33. Zhu, J.J.; Mao, Z.H.; Hu, L.L.; Zhang, J.X. Plant diversity of secondary forests in response to anthropogenic disturbance levels in montane regions of northeastern China. *J. Forest Res.* **2007**, *12*, 403–416. [CrossRef]
34. Huang, K.; Su, C.X.; Liu, D.W.; Duan, Y.H.; Kang, R.H.; Yu, H.M.; Liu, Y.Q.; Li, X.; Gurmesa, G.A.; Quan, Z.; et al. A strong temperature dependence of soil nitric oxide emission from a temperate forest in Northeast China. *Agric. For. Meteorol.* **2022**, *323*, 109035. [CrossRef]
35. Huang, S.N.; Elliott, M.M.; Felix, J.D.; Pan, Y.P.; Liu, D.W.; Li, S.L.; Li, Z.J.; Zhu, F.F.; Zhang, N.; Fu, P.P.; et al. Seasonal pattern of ammonium ^{15}N natural abundance in precipitation at a rural forested site and implications for NH_3 source partitioning. *Environ. Pollut.* **2019**, *247*, 541–549. [CrossRef] [PubMed]
36. Yang, K.; Zhu, J.J.; Yan, Q.L.; Sun, O.J. Changes in soil P chemistry as affected by conversion of natural secondary forests to larch plantations. *Forest Ecol. Manag.* **2010**, *260*, 422–428. [CrossRef]
37. Xi, D.; Bai, R.; Zhang, L.M.; Fang, Y.T. Contribution of anammox to nitrogen removal in two temperate forest soils. *Appl. Environ. Microbiol.* **2016**, *82*, 4602–4612. [CrossRef]
38. Li, S.L.; Gurmesa, G.A.; Zhu, W.X.; Gundersen, R.P.; Zhang, S.S.; Xi, D.; Huang, S.N.; Wang, A.; Zhu, F.F.; Jiang, Y.; et al. Fate of atmospherically deposited NH_4^+ and NO_3^- in two temperate forests in China: Temporal pattern and redistribution. *Ecol. Appl.* **2019**, *29*, e01920. [CrossRef]
39. Kaiser, J.; Röckmann, T.; Brenninkmeijer, C.A.M. Complete and accurate mass spectrometric isotope analysis of tropospheric nitrous oxide. *J. Geophys. Res.* **2003**, *108*, 4476. [CrossRef]
40. Buchen, C.; Lewicka-Szczebak, D.; Fuss, R.; Helfrich, M.; Flessa, H.; Well, R. Fluxes of N_2 and N_2O and contributing processes in summer after grassland renewal and grassland conversion to maize cropping on a Plaggic Anthrosol and a Histic Gleysol. *Soil Biol. Biochem.* **2016**, *101*, 6–19. [CrossRef]
41. Sgouridis, F.; Stott, A.; Ullah, S. Application of the ^{15}N gas-flux method for measuring in situ N_2 and N_2O fluxes due to denitrification in natural and semi-natural terrestrial ecosystems and comparison with the acetylene inhibition technique. *Biogeosciences* **2016**, *13*, 1821–1835. [CrossRef]
42. Spott, O.; Russow, R.; Apelt, B.; Stange, C.F. A ^{15}N-aided artificial atmosphere gas flow technique for online determination of soil N_2 release using the zeolite Kostrolith SX6 (R). *Rapid Commun. Mass Spectrom.* **2006**, *20*, 3267–3274. [CrossRef] [PubMed]
43. Baily, A.; Watson, C.J.; Laughlin, R.; Matthews, D.; McGeough, K.; Jordan, P. Use of the ^{15}N gas flux method to measure the source and level of N_2O and N_2 emissions from grazed grassland. *Nutr. Cycl. Agroecosyst.* **2012**, *94*, 287–298. [CrossRef]
44. Koba, K.; Hirobe, M.; Koyama, L.; Kohzu, A.; Tokuchi, N.; Nadelhoffer, K.J.; Wada, E.; Takeda, H. Natural ^{15}N abundance of plants and soil N in a temperate coniferous forest. *Ecosystems* **2003**, *6*, 457–469. [CrossRef]
45. Ullah, S.; Breitenbeck, G.A.; Faulkner, S.P. Denitrification and N_2O emission from forested and cultivated alluvial clay soil. *Biogeochemistry* **2005**, *73*, 499–513. [CrossRef]
46. Well, R.; Maier, M.; Lewicka-Szczebak, D.; Koster, J.R.; Ruoss, N. Underestimation of denitrification rates from field application of the ^{15}N gas flux method and its correction by gas diffusion modelling. *Biogeosciences* **2019**, *16*, 2233–2246. [CrossRef]
47. Scholefield, D.; Hawkins, J.M.B.; Jackson, S.M. Use of a flowing helium atmosphere incubation technique to measure the effects of denitrification controls applied to intact cores of a clay soil. *Soil Biol. Biochem.* **1997**, *29*, 1337–1344. [CrossRef]
48. Zaman, M.; Kleineidam, K.; Bakken, L.; Berendt, J.; Bracken, C.; Butterbach-Bahl, K.; Cai, Z.; Chang, S.X.; Clough, T.; Dawar, K.; et al. Isotopic techniques to measure N_2O, N_2 and their sources. In *Measuring Emission of Agricultural Greenhouse Gases and Developing Mitigation Options Using Nuclear and Related Techniques: Applications of Nuclear Techniques for GHGs*; Zaman, M., Heng, L., Müller, C., Eds.; Springer International Publishing: Cham, Switzerland, 2021; pp. 213–301.
49. Zhang, J.B.; Zhu, T.B.; Cai, Z.C.; Müller, C. Nitrogen cycling in forest soils across climate gradients in Eastern China. *Plant Soil* **2011**, *342*, 419–432. [CrossRef]
50. Houlton, B.Z.; Sigman, D.M.; Hedin, L.O. Isotopic evidence for large gaseous nitrogen losses from tropical rainforests. *Proc. Natl. Acad. Sci. USA* **2006**, *103*, 8745–8750. [CrossRef]
51. Bai, E.; Houlton, B.Z. Coupled isotopic and process-based modeling of gaseous nitrogen losses from tropical rain forests. *Global Biogeochem. Cycles* **2009**, *23*, GB2011. [CrossRef]
52. Fang, Y.T.; Koba, K.; Makabe, A.; Takahashi, C.; Zhu, W.X.; Hayashi, T.; Hokari, A.A.; Urakawa, R.; Bai, E.; Houlton, B.Z.; et al. Microbial denitrification dominates nitrate losses from forest ecosystems. *Proc. Natl. Acad. Sci. USA* **2015**, *115*, 1470–1474. [CrossRef] [PubMed]
53. Zhou, W.J.; Xi, D.; Fang, Y.T.; Wang, A.; Sha, L.Q.; Song, Q.H.; Liu, Y.T.; Zhou, L.G.; Zhou, R.W.; Lin, Y.X.; et al. Microbial processes responsible for soil N_2O production in a tropical rainforest, illustrated using an in situ ^{15}N labeling approach. *CATENA* **2021**, *202*, 105214. [CrossRef]